Video Article

Determination of the Relative Cell Surface and Total Expression of Recombinant Ion Channels Using Flow Cytometry

Benoîte Bourdin[1], Emilie Segura[1], Marie-Philippe Tétreault[1], Sylvie Lesage[2], Lucie Parent[1]

[1]Département de Physiologie Moléculaire et Intégrative, Montreal Heart Institute Research Centre

[2]Département de Microbiologie, Infectiologie, Immunologie, Centre de recherche de l'Hôpital Maisonneuve-Rosemont

Correspondence to: Lucie Parent at lucie.parent@umontreal.ca

URL: https://www.jove.com/video/54732
DOI: doi:10.3791/54732

Keywords: Cellular Biology, Issue 115, Calcium channels, cell surface protein expression, intracellular protein expression, recombinant expression, flow cytometry

Date Published: 9/28/2016

Citation: Bourdin, B., Segura, E., Tétreault, M.P., Lesage, S., Parent, L. Determination of the Relative Cell Surface and Total Expression of Recombinant Ion Channels Using Flow Cytometry. *J. Vis. Exp.* (115), e54732, doi:10.3791/54732 (2016).

Abstract

Inherited or *de novo* mutations in cation-selective channels may lead to sudden cardiac death. Alteration in the plasma membrane trafficking of these multi-spanning transmembrane proteins, with or without change in channel gating, is often postulated to contribute significantly in this process. It has thus become critical to develop a method to quantify the change of the relative cell surface expression of cardiac ion channels on a large scale. Herein, a detailed protocol is provided to determine the relative total and cell surface expression of cardiac L-type calcium channels $Ca_V1.2$ and membrane-associated subunits in tsA-201 cells using two-color fluorescent cytometry assays. Compared with other microscopy-based or immunoblotting-based qualitative methods, flow cytometry experiments are fast, reproducible, and large-volume assays that deliver quantifiable end-points on large samples of live cells (ranging from 10^4 to 10^6 cells) with similar cellular characteristics in a single flow. Constructs were designed to constitutively express mCherry at the intracellular C-terminus (thus allowing a rapid assessment of the total protein expression) and express an extracellular-facing hemagglutinin (HA) epitope to estimate the cell surface expression of membrane proteins using an anti-HA fluorescence conjugated antibody. To avoid false negative, experiments were also conducted in permeabilized cells to confirm the accessibility and proper expression of the HA epitope. The detailed procedure provides: (1) design of tagged DNA (deoxyribonucleic acid) constructs, (2) lipid-mediated transfection of constructs in tsA-201 cells, (3) culture, harvest, and staining of non-permeabilized and permeabilized cells, and (4) acquisition and analysis of fluorescent signals. Additionally, the basic principles of flow cytometry are explained and the experimental design, including the choice of fluorophores, titration of the HA antibody and control experiments, is thoroughly discussed. This specific approach offers objective relative quantification of the total and cell surface expression of ion channels that can be extended to study ion pumps and plasma membrane transporters.

Video Link

The video component of this article can be found at https://www.jove.com/video/54732/

Introduction

This paper provides a reliable assay to report the relative cell surface expression of membrane proteins such as ion channels expressed in recombinant cells using the existing flow cytometry technology. Ion channels are pore-forming membrane proteins that are responsible for controlling electrical signals by gating the flow of ions across the cell membrane. They are classified by the activation mechanism, nature, and selectivity of ion species transiting through the pore where they are localized. At the cellular and tissue levels, the macroscopic ion fluxes through ion channels are the product of biophysical (gating and permeation), biochemical (phosphorylation), and biogenesis (synthesis, glycosylation, trafficking, and degradation) properties[1]. Each of these processes is unique to every type of ion channels and is optimized to fulfill the physiological role of the ion channel. Consequently, alterations in any of these fine-tuned processes through an inherited or a genetic modification, often referred to as "channelopathy", can be detrimental to cell homeostasis. It is important to stress that delivering the "right" amount of ion channels at the cell surface is critical to cell homeostasis. Even small increases (gain-of-function) and small decreases (loss-of-function) in ion channel activity have the potential to cause a serious pathology over a lifetime. Defects in the cell surface delivery of mature ion channels is an important determinant in numerous channelopathies, such as cystic fibrosis (CFTR ion channel)[2] and cardiac arrhythmias of the long QT syndrome form (cardiac potassium channels)[3].

Channelopathies are associated with cardiac sudden death[4]. The current worldwide prevalence of all cardiac channelopathies is thought to be at least 1:2,000-1:3,000 per individual[5] and are responsible for about half of sudden arrhythmic cardiac death cases[6]. Dysfunction in cardiac voltage-gated sodium-, potassium-, and calcium- selective ion channels are known to play a key role in this process. The L-type $Ca_V1.2$ voltage-gated calcium channel is required to initiate synchronized heart muscle contraction. The cardiac L-type $Ca_V1.2$ channel is a multi-subunit protein complex composed of the main pore-forming $Ca_V\alpha1$ subunit and $Ca_V\beta$ and $Ca_V\alpha2\delta1$ auxiliary subunits[7-12]. Note that the full complement of auxiliary subunits is required to produce functional $Ca_V1.2$ channels at the plasma membrane and dynamic interactions between these subunits are essential to support the normal electric function of the heart[13]. $Ca_V\beta$ promotes the cell surface expression of $Ca_V1.2$ channels through a non-covalent nanomolar hydrophobic interaction[14]. Co-expression of the $Ca_V\alpha2\delta1$ subunit with $Ca_V\beta$-bound $Ca_V\alpha1$ stimulates peak

current expression (5 to 10-fold) and promotes channel activation at more negative voltages. Gain-of-function mutations of the pore-forming subunit $Ca_V1.2$ have been associated with a form of ventricular arrhythmias called the long QT syndrome[15] whereas a host of point mutations in the three main subunits forming the L-type $Ca_V1.2$ channel have been identified in subjects suffering from arrhythmias of the short QT syndrome form[16,17]. Ion channels are membrane proteins that can be investigated from a biochemical perspective (protein chemistry) or using electrophysiological tools (current-generating machines) and often using these complementary approaches. Electrophysiology, in particular whole-cell patch-clamping, is a suitable approach to elucidate the function of ion channels[15] but cannot resolve modifications in protein trafficking from changes in their biophysical properties. Protein chemistry has, however, often limited use due to the relatively low expression of large membrane proteins relative to smaller soluble proteins. Robust high-throughput methods using fluorescence readout need to be developed in order to specifically address defects in protein biogenesis causing changes in the cell surface expression of ion channels.

Flow cytometry is a biophysical technology employed in cell counting, sorting, biomarker detection, and protein engineering[18]. When a sample solution of live cells or particles is injected into a flow cytometer, the cells are ordered into a single stream that can be probed by the machine's detection system (**Figure 1**). The first flow cytometer instrument produced in 1956[19] detected only one parameter but modern flow cytometers have multiple lasers and fluorescence detectors that allow the detection of more than 30 fluorescent parameters[20,21]. Filters and mirrors (emission optics) direct the light scatter or fluorescent light of cells to an electronic network (photodiode and detectors) that convert the light proportionally to its intensity. Digital data are analyzed using specialized software and the primary output is displayed as a dot plot[21].

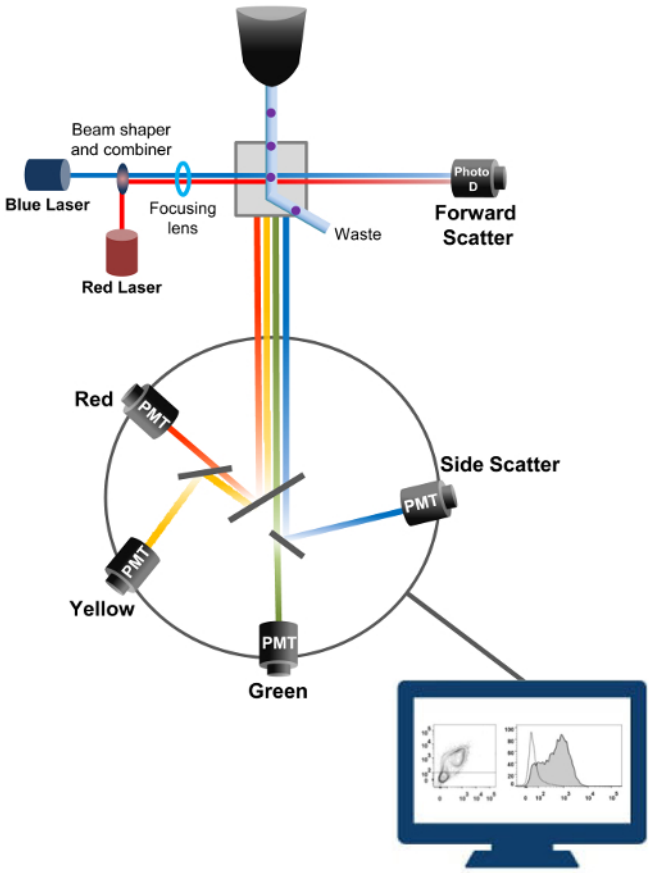

Figure 1: Biophysical principles of flow cytometry sorting. Single cells are pushed through a nozzle under high pressure within a stream of sheath fluid which moves them across one or more laser interrogation points. The light beam is deflected by the passing cells and the light collected in the forward direction (Forward Scatter, FCS) is sent to a photodiode that converts the light into a signal proportional to the size of the cell. The light is also collected at a 90° angle to the laser path and sent to detectors (also called photomultipliers (PMT)). This light is routed through dichroic mirrors that permit the detection of the side scatter signal (SSC), which reflects the granularity within the cells, and the fluorescent emissions if excited fluorochromes are present in the cell. Three detectors (Green, Yellow, and Red) are represented with different wavelength bandpass filters, allowing the simultaneous detection of different fluorochromes. The different signals are digitized by an external computer and converted into data that will be analyzed to quantify the characteristics of the cells. Please click here to view a larger version of this figure.

The high-throughput capacity of flow cytometers was exploited to quantify the relative membrane expression of recombinant wild-type and trafficking-deficient voltage-gated L-type $Ca_V1.2$ channels and associated subunits in live cells. cDNA constructs coding for the proteins were doubly tagged to simultaneously carry an extracellular non-fluorescent epitope that can be detected by an impermeable fluorescent conjugated antibody and an intracellular fluorophore that is constitutively fluorescent. Both the extracellular epitope, inserted in an extracellular loop of the protein, and the intracellular fluorophore, inserted after the C-terminus, are translated with the protein. In this series of experiments, the $Ca_V\alpha2\delta1$ protein was engineered to express an extracellular hemagglutinin (HA) epitope (YPYDVPDYA) detected by an impermeable FITC (Fluorescein isothiocyanate)-conjugated anti-HA and mCherry as the intrinsic intracellular fluorophore. To determine the relative cell surface expression level of the mCherry-$Ca_V\alpha2\delta1$ HA-tagged protein, recombinant cells expressing the fusion protein were harvested after transfection,

and stained with the FITC-conjugated mouse monoclonal anti-HA epitope tag antibody (**Figure 2**). FITC is an organic fluorescent compound that is considerably smaller than enzyme reporters and therefore not as likely to interfere with biological function. mCherry- $Ca_V\alpha2\delta1$-HA overexpressed in tsA-201cells, produces a significant 3-log increase in the FITC fluorescence and mCherry fluorescence on two-dimensional plots[22]. Given that the HA epitope is located in the extracellular portion of the protein, the fluorescence intensity for FITC obtained in the presence of intact cells reflect the relative index of the cell surface expression of HA-tagged protein. The accessibility of the HA epitope in the constructs is systematically validated by measuring the FITC signal after cell permeabilization. This measure also serves to corroborate the normalized total protein expression since the relative fluorescence intensities for FITC estimated in permeabilized cells are qualitatively comparable to the relative fluorescence values for mCherry measured under permeabilized and non-permeabilized conditions[22,23]. It is important to note that the intrinsic fluorescence spectrum is shifted toward higher values after permeabilization but that the only value being reported is the change in fluorescence intensity as compared to the control construct. Relative changes in the fluorescence intensity for the test constructs are estimated using the ΔMean Fluorescence Intensity (ΔMFI) values for each fluorophore (mCherry or FITC). Experiments are designed to measure the fluorescence intensity of the test construct relative to the fluorescence intensity of the control construct expressed under the same conditions to limit experimental variations in the intrinsic fluorescence of the fluorophore-conjugated antibody. Two membrane proteins were successfully studied using this assay: the pore-forming subunit of the L-type voltage-gated calcium channel $Ca_V1.2$[14,22] and in a different series of experiments, the extracellular auxiliary $Ca_V\alpha2\delta1$ subunit[22,23]. The following protocol was used to determine the cell surface expression of the $Ca_V\alpha2\delta1$ subunit of the cardiac L-type $Ca_V1.2$ channel under control conditions and after mutations affecting the posttranslational modification of the ion channel. Under standardized experimental conditions, the cell surface fluorescence of FITC increases quasi-linearly with the expression of cDNA coding for the mCherry-$Ca_V\alpha2\delta1$-HA proteins (**Figure 5** from reference[22]).

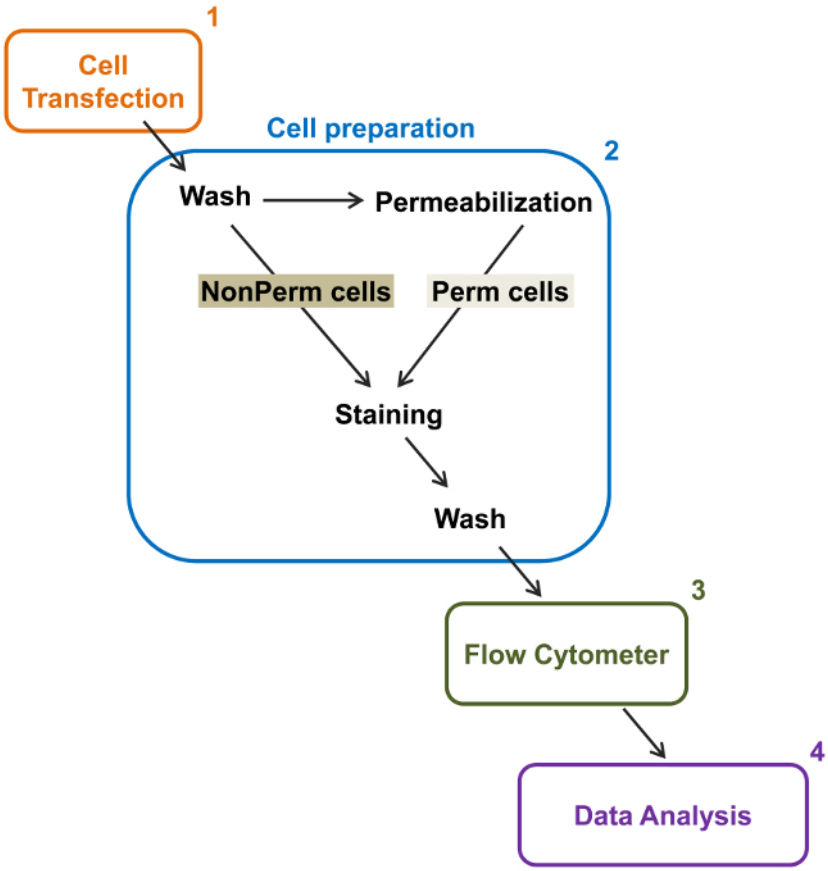

Figure 2: Schematic representation of total and membrane labeling in the flow cytometry experimental protocol. The scheme outlines some of the main steps necessary to quantify the relative total and cell surface expression of recombinant ion channels by flow cytometry. Cells are transfected with the double-tagged construction mCherry-$Ca_V\alpha2\delta1$-HA in tsA-201 cells (1) and stained before or after permeabilization (2). Multiparameter data are acquired in a flow cytometer (3) for multivariate analysis (4). Please click here to view a larger version of this figure.

Protocol

1. Doubly Tagged DNA constructs

1. Insert the HA epitope (YPYDVPDYA) in the extracellular linker of $Ca_V\alpha2\delta1$ between D676 and R677 by site directed mutagenesis (**Figure 3B**)[20]. Use Forward primer gccggattatgcgGGAAAACTCCAAACAACC and Reverse primer acatcatacggataTCAATAAATTCATTGAAATTTAAAAGAAATTC.
2. Subclone the cDNA sequence of the tagged HA $Ca_V\alpha2\delta1$ into the mammalian pmCherry-N1 expression vector designed to express the protein fused to the N-terminus of mCherry between the SacI and SalI sites (**Figure 3B**)[20].

NOTE: Appropriate channel function needs to be tested with the control construct using standard electrophysiological methods[24].

2. Liposome-mediated Transient Transfection (30 min, All Steps are Performed Under Laminar Flow Hood)

1. Day 1: Plate half a million of tsA-201 cells (or HEKT) in 35 mm culture dishes with 2 mL of Dulbecco's high-glucose minimum essential medium (DMEM-HG) supplemented with 10% Fetal Bovine Serum (FBS) and 1% penicillin-streptomycin (PS) culture medium. Count cells using a standard hemacytometer. Assess cell viability from a fraction of the cell sample using Trypan Blue. Plate enough cells to reach 90% confluence at the time of transfection.
2. Day 2: Change culture medium with 2 ml of fresh pre-warmed (37 °C) culture medium without PS.
3. For each transfection sample, prepare two 1.5 ml tubes. In tube 1, dilute 4 µg of DNA in 250 µl of reduced serum medium. In tube 2, mix 10 µl of the liposome-mediated transfection reagent with 250 µl serum-reduced culture medium. Mix gently the transfection reagent before use.
4. Incubate for 5 min at room temperature.
5. Combine the contents of tube 1 and tube 2, mix gently and incubate at least 20 min at room temperature.
6. Add the liposomes/DNA complexes to the cultured cells and gently rock the culture dish to mix.
7. Incubate at 37 °C under 5% CO_2 atmosphere for 24 hr.

3. Staining of Cells for Flow Cytometry (3 hr)

1. Preparing Cell Samples
    1. Day 3: Remove medium from the culture dish carefully and wash the cells with 400 µl of pre-warmed (37 °C) 0.05% trypsin-1x EDTA (ethylenediaminetetraacetic acid).
    2. Add 400 µl of trypsin-EDTA and incubate the dish at 37 °C under 5% CO_2 atmosphere for 5 min to allow cells to detach from the dish.
    3. Stop the enzyme digestion by adding 1 ml of cold culture medium without PS and wash out all the cells from the surface by pipetting gently 4-5 times. Avoid over-digestion and over-pipetting to reduce cell death.
    4. Collect cells in 1.5 ml tubes and place immediately on ice. Use ice cold solutions and keep the cells at 4 °C to prevent the internalization of surface antigens. Decrease lighting to limit photobleaching of the fluorescent signal.
    5. Centrifuge tubes at 400 x g for 5 min at 4 °C. Carefully aspirate and discard the supernatant.
    6. Re-suspend the pellet in 1 ml of phosphate-buffered saline 1x (PBS) to prepare a single cell suspension.
    7. Briefly vortex the tubes very gently and repeat steps 3.1.5 and 3.1.6 to completely remove culture medium.
    8. Re-suspend the pellet in 600 µl of 1x PBS and adjust the cell concentration to a minimum of 3 x 10^6 cells/ml.
    9. Divide the cells in two new 1.5 ml tubes for extracellular and intracellular staining. Include appropriate controls to discriminate specific staining from non-specific staining.
    NOTE: The isotype control antibody helps assessing the level of background staining and should ideally match each primary antibody's host species, isotype and fluorophore. Use isotype control and conjugated antibody at the same protein concentration.

Cell transfection / Antibody Staining	nontransfected cells	p-Cavα2δ-HA	pmCherry-Cavα2δ-HA
No antibody	Negative control	Negative control	Single color
Anti-HA isotype	Negative control	Negative control	Single color
Anti-HA FITC conjugated	Negative control	Single color	Double color

Table 1: **Flow-cytometry experiment control samples for non-permeabilized and permeabilized cells.** Each experiment needs to include the following negative controls: (1) Nontransfected cells (without antibody, with the isotype or with the conjugated antibody). (2) Transfected cells with the protein of interest subcloned in a plasmid without constitutive fluorescent intracellular fluorochrome (pCMV- Ca_Vα2δ1-HA) or with the doubly tagged construction (pmCherry-Ca_Vα2δ1 and incubated without antibody, with the isotype or with the conjugated antibody). Single color controls are used for compensation of fluorochrome emission overlap. The same controls are run for non-permeabilized and permeabilized conditions in each series of experiments.

2. Cell Surface Staining of Intact Live Cells
    1. Aliquot 1 x 10^6 cells/100 µl in 1.5 ml tubes.
    2. Add the FITC-conjugated monoclonal anti-HA antibody at 5 µg/ml and, vortex before incubating the cells on a rocker platform (200 rpm) in the dark at 4 °C for 45 min.
    NOTE: The optimal concentration of antibody was determined in preliminary titration experiments (**Figure 4**).
    3. Remove the cells from the dark and add 900 µl of 1x PBS/tube. Centrifuge at 400 x g for 5 min at 4 °C.
    4. Aspirate the supernatant and resuspend the pellet in 1 ml of 1x PBS, vortex and centrifuge at 400 x g for 5 min at 4 °C.
    5. Repeat the wash (step 3.2.4) twice to remove any unbound antibody. If an unconjugated primary antibody is used, incubate with the appropriate secondary antibody.
    6. After the final wash, resuspend the cells in 500 µl of 1x PBS and transfer the single cell suspension in 5 ml flow cytometry tubes. Keep the cells in the dark at 4 °C until running the sample.

7. Run the samples on a flow cytometer. For best results, analyze the cells on the flow cytometer as soon as possible and no later than 24 hr after.

3. Intracellular Staining: Fixation, Permeabilization, and Staining
    1. Aliquot 1 x 10^6 cells/100 µl in 1.5 ml tubes and centrifuge at 400 x g for 5 min at 4 °C.
    2. Discard supernatant and resuspend cells in 100 µl of fixation-permeabilization solution directly from stock.
    3. Incubate in the dark at 4 °C for 20 min.
    4. Add 100 µl of freshly prepared 1x permeabilization-washing buffer (dilute 10x permeabilization-washing buffer in distilled H_2O). Vortex and sediment cells using a table centrifuge at 400 x g for 5 min at 4 °C.
    5. Aspirate and discard the supernatant.
    6. Repeat steps 3.3.4 and 3.3.5.
    7. Add FITC-conjugated monoclonal anti-HA antibody at 5 µg/ml in 100 µl of 1x permeabilization-washing buffer and, vortex before incubating cells in the dark at 4 °C for 30 min.
       NOTE : The intracellular staining is performed following the same procedure as the one used for cell surface staining. Saponin-mediated cell permeabilization is however, a quickly reversible process, therefore it is important to replace 1x PBS with 1x Perm/Wash buffer to keep the cells in the constant presence of saponin during intracellular staining.
    8. Remove the cells from the dark and add 100 µl permeabilization-washing buffer. Centrifuge at 400 x g for 5 min at 4 °C.
    9. Aspirate carefully the supernatant and resuspend the pellet in 100 µl permeabilization-washing buffer, vortex and centrifuge at 400 x g for 5 min at 4 °C.
    10. Repeat the wash (step 3.3.9) one more time to remove any unbound antibody.
    11. After the final wash, resuspend the cells in 500 µl of 1x PBS and transfer the single cell suspension to 5 mL flow cytometry tubes. Keep the cells in the dark at 4 °C until injecting the sample into the flow cytometer.
    12. Run the samples on a flow cytometer. Run the fixed samples on the cytometer as soon as possible but no later than 1 week after staining. Run the non-permeabilized and permeabilized cells on the same day.

4. Flow Cytometry

1. Flow Cytometer Cell Sorter Daily Setup
    1. Turn on the flow cytometry software. Prior to experiment, calibrate and setup the flow cytometer cell sorter to ensure optimal instrument performance (*i.e.* laser and optics are performing to specification, the laser and flow cell are properly aligned) by using instrument setup beads.
    2. Use the 100 µm nozzle with 20 psi sheath pressure.
       NOTE: The nozzle does not have to be changed on a bench flow cytometer.
    3. Set the cytometer's flow rate according to the manufacturer specification. Exceedingly high flow rates will decrease sensitivity in the detection of variations in fluorescence.
    4. Select blue (488 nm to excite Fluorescein Isothiocayanate or FITC) and yellow-green (561 nm to excite mCherry) lasers. Collect FITC and mCherry fluorescence levels with a 530/30 nm and with a 610/20 nm bandpass filter respectively.
    5. Acquire the forward scatter (FCS) versus side scatter (SSC) dot plot for unstained cells using linear scale. Adjust each detector's amplification to visualize cells in the lower left quadrant of the dot plot.

2. Sample Reading of Intact Non-permeabilized Cells
    1. Set the P1gate for live non-permeabilized cells by delineating a free form around the cells to be analyzed excluding cell debris and cell aggregates, thus limiting the fluorescence signal to intact cells.
       NOTE: Live/dead exclusion dyes can be used to facilitate gate placement on live cells. Set 10,000 events to record in the stopping gate P1. Set this to a higher number of events if need be.
    2. Acquire mCherry versus FITC two-parameter contour plot to detect baseline autofluorescence of unstained cells. Use bi-logarithmic scale to show negative values and improve resolution between populations[25]. Adjust each detector's voltage to set the unstained negative cells within the lower portion of the first ten units of the log fluorescence intensity plots.
    3. Acquire all intact non-permeabilized samples using settings established in 4.1.5 and 4.1.6 and collect FSC, SSC and signals in the fluorescence detectors.
    4. Export and save *.fcs files to be used for analysis using flow cytometry analysis software.

3. Sample Reading of Permeabilized Cells
    1. Move the P1 gate to select live cells in the permeabilized samples and adjust FSC and SSC voltage as shown in 4.1.5 and 4.1.6.
    2. Acquire all permeabilized samples and collect FSC, SSC and signals in the fluorescence detectors.
    3. Export and save *.fcs files to be used for analysis using flow cytometry analysis software.

4. Data Analysis
    1. Launch the flow cytometry analysis software and import *.fcs files saved in 4.2.4 and 4.3.3.
    2. Click on the first sample listed in the workspace window. A new window named after the tube I.D. number opens automatically. Start the gating process in the plot of SSC versus FSC. Draw a gate (P1) using the Ellipse icon around live cells and eliminate any debris, dead cells, or aggregates which have different forward scatter and side scatter than live cells
    3. To draw the two-parameter contour plot of the mCherry (y-axis) versus FITC (x-axis) fluorescence intensity of the live cells, click first on the x-axis and choose the FITC-A channel and then click on the y-axis and choose the PE-mCherry-A channel. Click on the "Quad" icon to position the quadrant marker at the edge of autofluorescent cells in each fluorescence channel.
       NOTE: The gate set around the FITC and mCherry positive cells is the P2 gate. The fluorescence negative cell population is referred to as the P3 gate. See **Figure 5** for the representative gating method used in this article.
    4. Select P2 and P3 gates and click on the "Add Statistics" icon in the original workspace window. Click on "Count" (number of positive cells) and click on "Mean" (Mean Fluorescence Intensity of each fluorochrome) or "Median" (Median Fluorescence Intensity of each

fluorochrome) statistics among the list of options. Click on the "Add Statistics" icon again. All these values are automatically transferred to the original workspace window.
NOTE: The "Mean" is used only if the fluorescence intensity follows a normal distribution. In every other case, click on the "Median" tab. MFI thus could refer to Mean Fluorescence Intensity or Median Fluorescence Intensity.
NOTE: The next step is to apply the gates' parameters and statistics to all samples probed by the cytometer.

5. In the workspace window, use the mouse to drag and drop the gates and statistics parameters onto the line marked ALL SAMPLES.
6. Generate a batch report of two-dimensional contour plots (mCherry vs FITC) and histograms (cell count versus fluorescence intensity) for non-permeabilized and permeabilized cells (**Figures 6A**-**B**).
7. From the statistics generated in step 4.4.4, calculate the mean fluorescence intensity (MFI) for each fluorochrome for the stained cells. From this value, subtract the MFI value obtained from unstained cells to quantify the surface and total expression of the protein of interest.
8. Report the ΔMFI values for each fluorophore (mCherry and FITC) (**Figure 6C**-**D**). Normalize the ΔMFI measured for the $Ca_V\alpha2\delta1$ construct mutants to the ΔMFI value obtained for FITC and mCherry with the WT construct.
NOTE: The absolute value of fluorescence intensity could vary sharply depending upon the batch of antibodies and the technical abilities of each lab worker, hence the need to normalize fluorescence intensity of the mutant construct using the WT construct.

Representative Results

This article describes a reliable protocol to quantify total and cell surface of recombinant ion channels expressed in tsA-201cells by a two-color flow cytometry assay. As an example, the relative cell surface and total protein expression was quantified for the $Ca_V\alpha2\delta1$subunit. In order to perform the two-color flow cytometry assay, $Ca_V\alpha2\delta1$ was doubly tagged to express an extracellular non-fluorescent epitope HA that can be detected by an anti-HA FITC-conjugated antibody and a constitutive fluorescent intracellular mCherry fluorophore. The excitation and emission spectra for FITC and mCherry show that FITC is excited with 88% efficiency by the 488 nm laser but efficiency decreases to 0% with the 561 nm laser. The mCherry shows 63.9% of its maximum fluorescence when excited with the 561 nm laser but only 7.6% with the 488 nm laser (**Figure 3**). The excitation and emission spectra for both fluorophores exhibit optimal light collection and minimal overlap with the different lasers and filters selected. Flow cytometry assays could provide quantitative information about the relative expression of membrane proteins from a large cell population as long as the MFI for the given fluorochrome is directly proportional to the protein expression of $Ca_V\alpha2\delta1$ on each cell rather than the number of fluorescent cells. This involves using a concentration of fluorescence-conjugated antibody beyond saturation. The titration curve for the anti-HA FITC-conjugated antibody binding to $Ca_V\alpha2\delta1$ (**Figure 4**) shows three phases. While no fluorescence was detected in the first phase, the fluorescence intensity increased exponentially with increasing antibody concentration in the second phase. After the point of saturation (third phase), increasing the concentration of the antibody has no effect on the relative fluorescence intensity (RFI) of FITC. The anti-HA FITC-conjugated antibody saturation point was established at 5 µg/ml, thus ensuring that the concentration of the conjugated-antibody is not limiting the MFI during the experiments.

The tagged $Ca_V\alpha2\delta1$was expressed in tsA-201cells and flow cytometry assays were carried out in the presence of the FITC-conjugated anti-HA in non-permeabilized cells (**Figure 5**). Appropriate controls (**Table 1**) were analyzed on the flow cytometer that attributes x-y values to each cell passing through the laser beam. The cell distribution is visualized on dot plots (**Figure 5A**). FCS/SSC dot plots confirm that the preparation of cell samples provides a single cell suspension with high viability (**Figure 5Ba**). The selected gate for live cells (P1) represents 75% of the total number of cells analyzed. The total protein expression of $Ca_V\alpha2\delta1$ in tsA-201 cells was considered to be proportional to the mCherry fluorescence. As seen in the mCherry *versus* FITC contour plots and histograms (**Figure 5Bb**-**Bc**), 47 2% tsA-201 cells transfected with pmCherry-$Ca_V\alpha2\delta1$-HA were found to significantly express mCherry fluorescence as well as showing significant FITC fluorescence due to the binding to the external HA tag of $Ca_V\alpha2\delta1$ in non-permeabilized cells. Negative control experiments carried out without antibody or with the isotype indicate that the FITC binds only or mostly to the positively transfected cells.

This protocol was used to characterize the role of N-glycosylation on total and cell surface expression of $Ca_V\alpha2\delta1$ in tsA-201cells[23]. Experiments were carried out in non-permeabilized cells to assess the cell surface expression and in permeabilized cells to evaluate the total protein expression as well as confirming the accessibility of the HA epitope. Relative expression of $Ca_V\alpha2\delta1$ was calculated based upon the MFI estimated for each fluorophore (mCherry or FITC). ΔMFI values for the mutants were normalized to the maximum value measured the same day for mCherry-$Ca_V\alpha2\delta1$-HA WT expressed under the same conditions. This is important to account for variations over time in the absolute fluorescence intensity of the anti-HA FITC conjugated antibody. As seen in **Figure 6A**, the ΔMFI for FITC in non-permeabilized cells was strong for the WT and the 4xNQ construct but close to the background fluorescence level for the 16xNQ construct indicating that the protein is nearly absent from the plasma membrane. Assays conducted after cell permeabilization, showed that total protein expression of the 16xNQ construct was also significantly decreased whether it was inferred from the FITC fluorescence in permeabilized cells or from the constitutive mCherry fluorescence measured in non-permeabilized and in permeabilized cells (**Figure 6C**-**D**). As seen in **Figure 6B**, the cellular autofluorescence levels increased after cell permeabilization, which prevents comparison of the absolute fluorescence values between intact non-permeabilized and permeabilized cells. The ΔMFI fluorescence measured for mCherry was similar for both non-permeabilized and permeabilized cells signifying that the permeabilization solution does not alter the relative fluorescence signal of mCherry. Mutations of the N-glycosylation sites was associated with a decrease in the fluorescence intensity for mCherry supporting the published observation that the protein biogenesis/stability was reduced[23]. In this series of experiments, the relative fluorescence signal for FITC measured in permeabilized cells turned out to be even smaller than the relative signal for mCherry suggesting that the N-type glycosylation status of the protein could influence the fluorescence intensity detected by the FITC-conjugated anti-HA antibody in the extracellular domain. Altogether the changes in the relative fluorescence of FITC before after cell permeabilization provide a reliable metric to quantify protein expression.

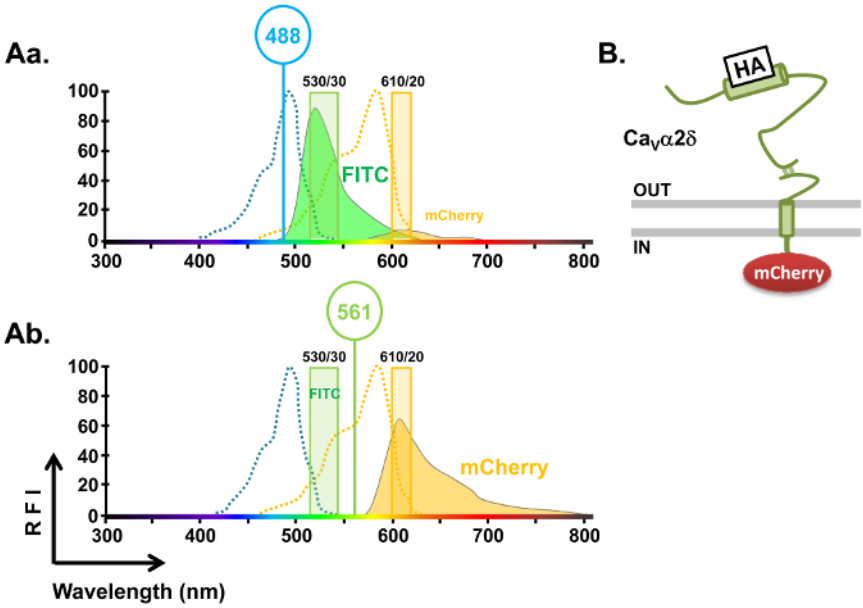

Figure 3: FITC and mCherry form a suitable pair of fluorochromes for two-color cytometry assays. Excitation (empty curves) and emission spectra (filled curves) for FITC excited with 488 nm blue laser (**Aa**) and mCherry excited with 561 nm yellow-green laser (**Ab**). FITC and mCherry fluorescence were collected with a 530/30 nm and a 610/20 nm bandpass filters respectively. The wavelength of the different lasers (colored vertical lines) and the filters (colored rectangles) are chosen for optimal light collection and minimal overlap. (**B**) Schematic representation of mCherry-Ca$_V$α2δ1-HA protein. Ca$_V$α2δ1 was doubly tagged to express an extracellular non-fluorescent epitope HA that can be detected by an anti-HA FITC-conjugated antibody and a constitutive fluorescent intracellular mCherry fluorochrome. Please click here to view a larger version of this figure.

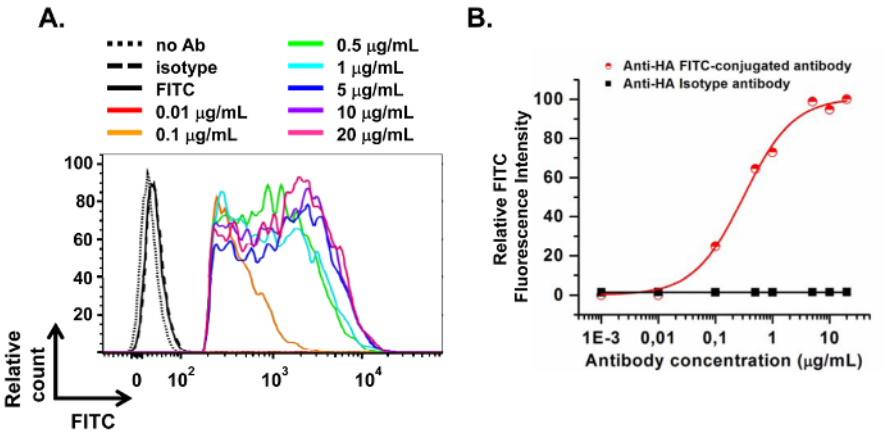

Figure 4: Titration of anti-HA FITC-conjugated monoclonal antibody binding to Ca$_V$α2δ1. tsA-201 cells were transiently transfected with pmCherry-Ca$_V$α2δ1-HA and incubated with a range of anti-HA FITC-conjugated or isotype antibodies. Only the FITC signal is being analyzed in this panel. (**A**) Single-parameter histograms display the relative number of cells on the y-axis and the FITC fluorescence intensity on the x-axis for the anti-HA FITC-conjugated antibody range of concentrations (0.01-20 µg/ml). (**B**) Semi-log graph for the anti-HA FITC-conjugated antibody as a function of the MFI of FITC. The titration curve was fitted using One Site Binding equation with a trendline value R^2 = 0.99561. Titration performed for the isotype antibody showed no fluorescence as expected. The concentrations from 0.001 to 0.01 µg/ml are indistinguishable from the background noise. Please click here to view a larger version of this figure.

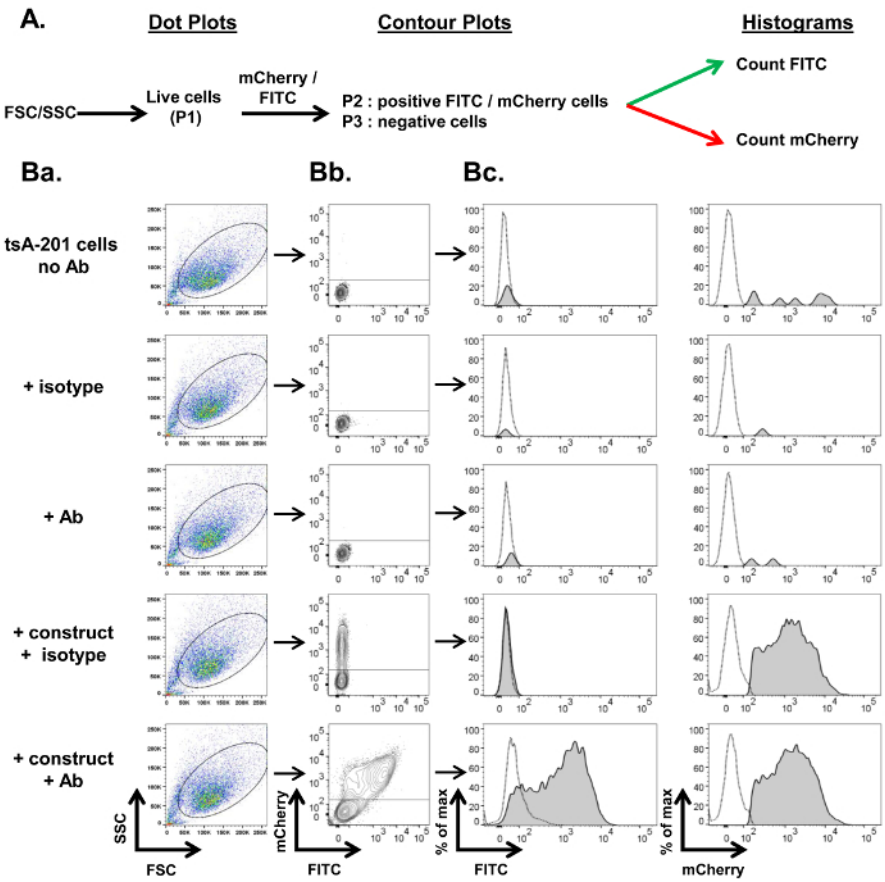

Figure 5: Representative flow cytometry analysis of non-permeabilized tsA-201cells transfected with pmCherry-$Ca_V\alpha2\delta1$-HA. (**A**) Schematic representation of gating strategy used in flow cytometry analysis sample. Data were analyzed after acquisition with the appropriate software. The first gating strategy exploits a forward scatter (FSC) and side scatter (SSC) dot plot to display a gate (P1) around live cells and eliminate any debris, dead cells, or aggregates which have different forward scatter and side scatter than live cells. Two-parameter contour plots of the mCherry (y-axis) *versus* FITC (x-axis) fluorescence intensity were displayed for the P1 population. Rectangular gates were placed at the edge of the autofluorescence of cells to select the positive population P2 (FITC and mCherry) and the negative population P3. The level of fluorescence for the cells within the region P2 and P3 were visualized using subsequent cell count *versus* FITC or mCherry fluorescence intensity single-parameter histograms. A shift in the fluorescence intensity on the y- and x-axis provides a reliable index of the total and membrane expression of $Ca_V\alpha2\delta1$ respectively. The intensity of the fluorescence signal increases as a function of the number of fluorochrome molecules. (Ba) Representative FCS/SSC dot plots for each condition as stated. A total of 10,000 events were acquired for analysis. The ellipse gate (P1) is drawn by eye around live cells excluding events with low FSC (dead cells) or high SSC (aggregates). (Bb) Representative two-parameter contour plots of the mCherry (y-axis) *versus* FITC (x-axis) fluorescence intensity. Gates were placed at the edge of autofluorescence of the cells to segregate populations of FITC-mCherry positive cells (P2 gate) and negative fluorescent cells (P3). (Bc) Single-parameter histograms of relative count (or % of max) cells *versus* fluorescence intensity (FITC or mCherry). The distribution of the fluorescence intensity measured for cells within the P2 gate (fluorescence-positive cells) are shown in *gray,* and the distribution of fluorescence intensity for cells present in the P3 gate (fluorescence-negative cells) is displayed as an overlay in a transparent *gray plot*. As seen, the fluorescence intensity was strong for both mCherry and FITC indicating that $Ca_V\alpha2\delta1$ is well expressed and clearly present at the cell membrane. Please click here to view a larger version of this figure.

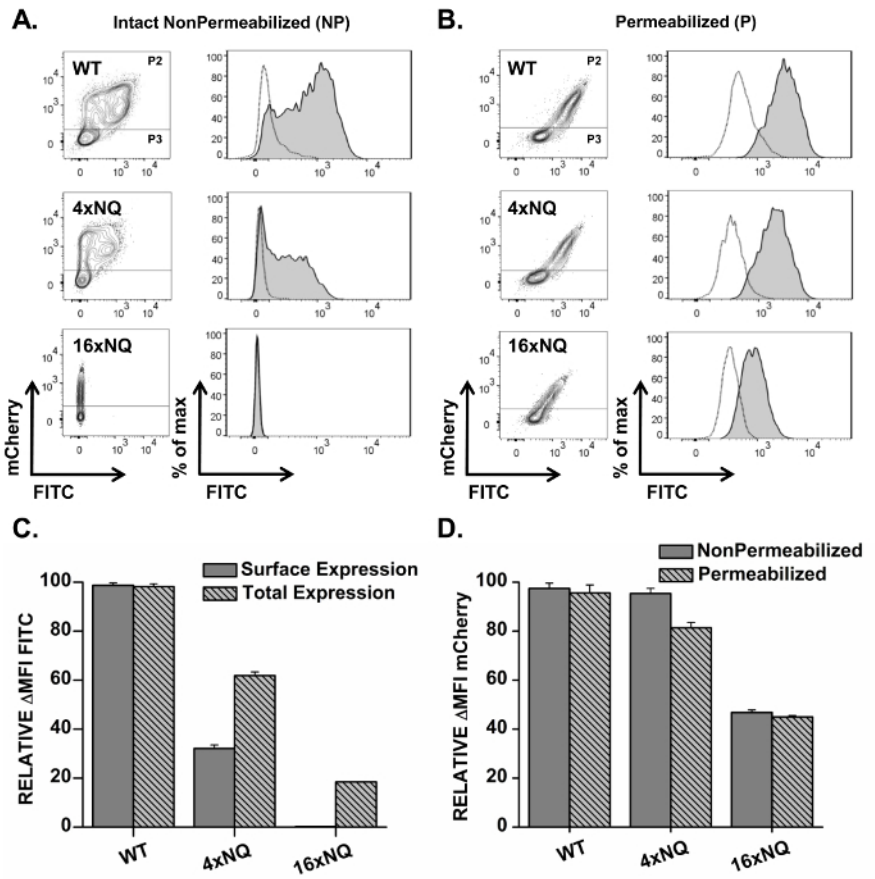

Figure 6: Simultaneous mutations of *N*-glycosylation sites disrupted cell surface expression of $Ca_V\alpha2\delta1$. Stable tsA-201 $Ca_V\beta3$ cells were transiently transfected simultaneously with pCMV-$Ca_V1.2$ WT and pmCherry-$Ca_V\alpha2\delta1$-HA WT or mutants. Non-permeabilized (**A**) and permeabilized cells (**B**) were stained with anti-HA FITC-conjugated antibody as described above. Representative two-parameter contour plots of mCherry *versus* FITC fluorescence (left panels) and histogram plots of the distribution of the fluorescence intensity for the anti-HA FITC conjugated antibody staining (right panels) are shown for *N*-glycosylation mutants (NQ) after the disruption of four sites (4xNQ: N92Q/ N184Q/ N468Q/ N876Q) and 16 sites (16xNQ: N92Q/ N136Q/ N184Q/ N324Q/ N348Q/ N468Q/ N475Q/ N585Q/ N594Q/ N663Q/ N769Q/ N812Q/ N876Q/ N883Q/ N973Q/ N986Q) in intact non-permeabilized or NP cells (**A**) and in permeabilized or P cells (**B**). The distribution of the fluorescence intensity measured for cells within the P2 gate (fluorescence-positive cells) are shown in *gray,* and the distribution of fluorescence intensity for cells present in the P3 gate (fluorescence-negative cells) is displayed as an overlay in a transparent *gray plot*. As seen in (**B**), the autofluorescence levels increased after cell permeabilization. The fluorescence intensity for FITC measured for all transfected permeabilized cells increased (seen as a right-shift on the x-axis) indicating that all transfected HA-tagged $Ca_V\alpha2\delta1$ proteins were stained and detected by the anti-HA FITC antibody. (**C**) Bar graph shows the normalized MFI measured in the presence of FITC in intact non-permeabilized (surface expression) or permeabilized cells (total expression). The relative fluorescence density was measured in triplicates for each condition (30,000 cells) and in three different batches of cells transfected over a period of 1 month hence the data are shown as the mean ± SEM for 90,000 cells for each condition. The peak fluorescence intensity was reached between 24 and 36 hr after transfection. The ΔMFI values for FITC measured in intact non-permeabilized cells was used as an index of the cell surface expression of $Ca_V\alpha2\delta1$-HA, and ΔMFI values for FITC measured in permeabilized cells reflect the total protein expression (cell surface and intracellular protein expression). ΔMFI for FITC was calculated by subtracting the FITC fluorescence intensity of the FITC negative cells (P3) from the fluorescence intensity of the FITC positive cells (P2). The same method was used to calculate the ΔMFI for mCherry. MFI values were normalized to the maximum value measured the same day for mCherry-$Ca_V\alpha2\delta1$-HA WT. (**D**) Bar graph shows the normalized ΔMFI mCherry measured in non-permeabilized or permeabilized cells (total expression). Results are expressed as mean ± S.E.M. Please click here to view a larger version of this figure.

Discussion

This flow cytometry-based assay was successfully applied to the measurement of relative total and cell surface levels of fluorescently-labelled pore-forming and associated subunits of voltage-gated calcium channels[14,22,26]. It is best used when investigating the impact of genetic mutations and thus requires that the intrinsic fluorescence intensity of the fluorescently-labelled tagged wild-type construct be at least 10 to 100-fold larger than for the fluorescence intensity of the fluorescently-labelled untagged construct. In this particular instance, the mCherry-$Ca_V\alpha2\delta1$-HA construct described herein yielded a larger signal to noise ratio and a larger dynamic range than what was measured for the previously published $Ca_V1.2$-HA and $Ca_V2.3$-HA constructs. There are many conceivable reasons for this. It can be speculated that the local environment of the HA epitope in the extracellular domain of the $Ca_V\alpha2\delta1$ protein maximizes the signal to noise ratio of the FITC-conjugated anti-HA antibody.

In addition, it is important to keep in mind that this method does not provide an absolute value in the number of proteins at the cell surface. The relative expression of the tagged construct required to obtain functional channel expression can be obtained nonetheless by performing side by

side patch-clamp and flow cytometry experiments under the same conditions as shown in **Figure 7** of reference[22]. From these data, it can be estimated that the peak current density, a global measure of ion channel activity, generally increases as a function of the surface expression of the tagged $Ca_V\alpha2\delta1$ subunit. The major limitation of this current cell surface expression assay remains that it cannot be applied at this time to the study of endogenous ion channels. This is due to the fact that few commercially available antibodies are known to specifically bind to predicted external domains of ion channels. It thus requires genetic manipulation of the primary sequence of the protein to be studied expressed in an undifferentiated recombinant cell line such as tsA-201 cells.

Critical steps in the optimization of the assay: The identification of the appropriate pair of fluorophores, the choice of the external epitope, and the localization of the insertion site are crucial to the success of this method because the insertion of the epitope should not interfere with protein function. Different fluorophore combinations were tested. Two external epitopes: the hemagglutinin (HA) epitope (YPYDVPDYA) and the bungarotoxin-binding-site epitope (WRYYESSLEPYPD)[27] and three impermeable fluorescent conjugated antibodies were evaluated, namely the FITC (Fluorescein isothiocyanate) -, the R-phycoerythrin -, and the PE-Cy7- conjugated-antibodies. In addition, more than 10 different insertion sites for the external HA epitope were tested within $Ca_V\alpha2\delta1$. In regard to the insertion of the epitope that requires site-directed mutagenesis and recombinant DNA techniques, it is advised to design a minimum of three sets of primers within the same region. With 9 residues, the HA epitope is one of the smaller epitopes for which exists commercially available fluorescent-conjugated antibodies but the success rate of inserting 27 nucleotides is lower than for point mutation. Tetracysteine motifs (residues Cys-Cys-Pro-Gly-Cys-Cys) are 2-residue smaller than the HA epitope but the fluorescein arsenical hairpin binder is membrane permeant and not suitable for the analysis of membrane-bound proteins[28]. Preliminary experiments were conducted with two intracellular fluorophores mCherry and Green Fluorescent Protein (GFP). Three criteria were used to discriminate the successful pair of fluorophores with ion channels: 1) emission spectra of the fluorophores needs not to overlap (see references[20,21] for details); 2) the expression of the tagged construct generates functional ion channel in recombinant cells as validated by standard electrophysiological methods; and 3) the expression of the control construct produces a robust fluorescent readout. If one of these criteria is not fulfilled, for instance if the insertion of the tag or the fluorophore interferes with channel function, one has to go back to square one and modify either the site of insertion of the external epitope and/or the insertion site of the fluorophore. A linker of 5-glutamine residues between the C-terminal of the protein and the fluorophore could help to improve protein function. In addition, it might help to insert the external epitope in large loops that are not known to play a critical role in protein function and/protein glycosylation. One also needs to be aware of minor technical aspects.

The success rate of liposome-mediated transfection in tsA-201 cells could be decreased after the insertion of the two epitopes within $Ca_V\alpha2\delta1$. Hence it is suggested to recalibrate the transfection efficiency with the novel DNA constructs. This happens because the insertion of a 30 kDa protein changes the molecular weight of the DNA. One could modify the DNA to liposomes ratio to 1:2 to 1:3 if necessary or incubate the cells at 37 °C for a longer period of time (24-72 hr). It is important to choose the right formulation for permeabilizing the cells. Most homemade solutions appraised for this project turned out to cause the cells to aggregate and clog the flow cytometer.

Curbing light exposure while staining the cell with the fluorophore conjugated antibody is essential to limit photobleaching and loss of signal. To minimize fluorescent background, it is important to centrifuge the excess of conjugated antibody before use. Finally, it is of the uttermost importance to analyze the cells on the flow cytometer as soon as possible as and no later than 24 hr after. Keeping the stained cells overnight at 4 °C will likely reduce the signal and impair cell survival. Variations in the intrinsic fluorescence of the fluorophore-conjugated antibody from batch to batch dictate that the fluorescence intensity of the test construct needs to be reported as a function of the fluorescence intensity of the control construct expressed under identical experimental conditions.

To achieve an overall good signal to noise ratio, it is recommended to minimize cell pipetting to reduce cell death and to gently resuspend the cells such that a 3×10^6 cells/ml are injected in the flow cytometer. Beware that a higher cell concentration will reduce the cell flow and could clog the flow cytometer. On the other hand, a lower cell concentration will require a longer processing time. One may thus have to adjust the concentration depending upon the type of cells to be analyzed.

Alternative assays: Additional methodologies deployed to document the presence of ion channels at the cell surface plasma membrane fall in four large categories: 1) Confocal imaging methods exploiting the high-affinity interaction between the fluorophore-conjugated antibodies and the target protein; 2) Protein chemistry techniques resting on the covalent modification of the target protein by biotinylation reagents; 3) Electrophysiological measures of non-stationary noise analysis; and 4) Photoaffinity labeling of the target protein with radioactive probes. In the case of the voltage-gated calcium channel, photoaffinity labeling with tritiated (±)-[^{3}H]PN 200-100, a high-affinity ligand of the dihydropyridine family was used extensively in the 1980s[31]. It remains a highly sensitive assay but involves the manipulation of radioactive material[31], which has fallen out of fashion following the advent of highly sensitive fluorescence and luminescence probes especially with younger investigators. In addition, it is impossible to measure ion channel activity in the presence of the antagonist, such that the correlation between surface expression and function is beyond the scope of this approach. At the other end of the experimental continuum, non-stationary noise analysis of ion channels requires high quality gigaseal patch-clamp recordings with stable baseline for minute-long recordings. With this approach one can extract the number of open ion channels in a single cell from the slope of the graphic plotting the noise variance as a function of the average current measured at any given potential[32-34]. It displays the same trappings of standard electrophysiological approaches. It is a labor-intensive and low-throughput method that requires in addition a good familiarity with spectral analysis[32-34], not a staple of cell biologists. Furthermore, this type of analysis identifies the number of active ion channels (in the open state) which might be different than the number of total proteins at the membrane. Labeling of cell surface proteins with biotin reagents is a relatively efficient tool to identify proteins present at the plasma membrane. This method exploits the covalent modification of membrane proteins by biotin and further high-affinity and high-specificity non-covalent binding of biotin to membrane-impermeant streptavidin or avidin molecules. This approach is qualitatively reliable but is hampered or limited by quantification issues regularly associated with revealing proteins using the western blot technique. Confocal imaging and its derivatives are widely used to document the co-localization of membrane proteins with the cell surface[35]. Qualitative plasma membrane isolation remains possible using differential centrifugation techniques with or without sucrose gradient[36]. As in the above-described flow cytometry assay, it relies upon the highly specific interaction between the target protein and a fluorophore-conjugated antibody. Total internal reflection fluorescence imaging in particular, is a powerful approach that could report the distribution and molecular behavior of single ion channels at the membrane surface[37,38]. The readout is definitely eye-catching but remains a low-throughput small-volume approach. All of those assays have their scientific merit. The high-throughput flow cytometry-based assay is superior in terms of readout reproducibility and quantifiable metrics but requires easy access to multi-laser flow cytometry cell sorters that are part of core facilities in large institutions. Fluorescence-based plate readers are cheaper

and more accessible but the signal to noise ratio obtained measured with the same constructs under the same experimental conditions was significantly lower due in large part to a higher fluorescence background. Cost of the fluorophore-conjugated antibodies can also be factored in especially due to the number of appropriate control experiments that have to be processed with the test constructs. Variations on the same theme include changing the fluorescent dye-conjugated antibody to cost-effective horse-radish peroxidase or alkaline phosphatase enzyme reporter antibodies which enzyme activity can be assayed by chemiluminescence[29,30].

Conclusion: Two-color fluorescence assays were developed to estimate the relative cell surface expression of recombinant proteins expressed in cultured cells using flow cytometers. Although only two fluorescent parameters were used in this current assay, flow cytometry is amenable to the simultaneous detection of more than 30 fluorescent probes on a single cell, demonstrating the high flexibility of this approach. This high-throughput ultrasensitive assay can be adapted to investigate the impact of genetic mutations[22,26] or posttranslational modifications[23], as well as studying the pharmacological profile of chaperones for the surface trafficking of membrane proteins techniques[39]. The impetus behind this protocol arose from the need to evaluate in isolation the impact of genetic mutations on the membrane expression of ion channels in recombinant cells. It is however important to note that the severity of mutant channel dysfunction in model cell lines does not always correlate with the severity of clinical symptoms in mutation carriers[5] in part because a combination of mutations in different alleles might be required to trigger sudden cardiac death[40,41]. In this context, this assay can be seen as providing a rapid first-step approximation of studying single or multiple mutations in a single gene associated with loss-of-function mutations[22]. It is however plausible to envision in the future the virus-mediated expression of the same constructs in differentiated cells of cardiomyocyte lineage. Overall, as compared with other imaging or luminescent techniques, flow cytometer sorters handle live cells in suspension and report fluorescence intensity of a homogeneous cell population. This process is done without the need for fixation with paraformaldehyde, a process that induces local plasma membrane permeabilization, even under mild conditions[42]. The assay is rapid, specific, and convenient with the analysis of up to several hundred samples per working day. In addition to analysis, the cells may eventually be sorted by flow cytometry to assess the functional potential of cells expressing higher or lower levels of the same membrane protein.

Disclosures

The authors declare that they have no competing financial interests.

Acknowledgements

We thank Mr. Serge Sénéchal and Dr. Jacques Thibodeau for sharing their expertise and granting us access to their flow cytometry and cell sorting platform. This work was completed with the operating grant 130256 from the Canadian Institutes of Health Research, a grant-in-aid from the Canadian Heart and Stroke Foundation, and support from the "Fondation de l'Institut de Cardiologie de Montréal" to L.P.

References

1. Delisle, B.P., Anson, B.D., Rajamani, S., & January, C.T. Biology of Cardiac Arrhythmias: Ion Channel Protein Trafficking. *Circ. Res.* **94,** 1418-1428, (2004).
2. Birault, V., Solari, R., Hanrahan, J., & Thomas, D.Y. Correctors of the basic trafficking defect of the mutant F508del-CFTR that causes cystic fibrosis. *Curr Opin Chem Biol.* **17**, 353-360, (2013).
3. Balijepalli, S.Y., Anderson, C.L., Lin, E.C., & January, C.T. Rescue of Mutated Cardiac Ion Channels in Inherited Arrhythmia Syndromes. *J. Cardiovas Pharm.* **56,** 113-122 (2010).
4. Gargus, J.J. Unraveling Monogenic Channelopathies and Their Implications for Complex Polygenic Disease. *Am. J. Hum. Genet.* **72,** 785-803 (2003).
5. Abriel, H., & Zaklyazminskaya, E.V. Cardiac channelopathies: Genetic and molecular mechanisms. *Gene.* **517,** 1-11 (2013).
6. Behr, E.R. *et al.* Sudden arrhythmic death syndrome: familial evaluation identifies inheritable heart disease in the majority of families. *Eur Heart J.* **29,** 1670-1680, (2008).
7. Catterall, W.A. Structure and regulation of voltage-gated Ca^{2+} channels. *Annu. Rev. Cell Dev.Biol.* **16,** 521-555, (2000).
8. Peterson, B.Z., DeMaria, C.D., Adelman, J.P., & Yue, D.T. Calmodulin is the Ca^{2+} sensor for Ca^{2+} -dependent inactivation of L- type calcium channels. *Neuron.* **22,** 549-558 (1999).
9. Dolphin, A.C. Calcium channel diversity: multiple roles of calcium channel subunits. *Curr.Opin.Neurobiol.* **19,** 237-244 (2009).
10. Dai, S., Hall, D.D., & Hell, J.W. Supramolecular assemblies and localized regulation of voltage-gated ion channels. *Physiol Rev.* **89,** 411-452 (2009).
11. Gao, T. *et al.* Identification and subcellular localization of the subunits of L-type calcium channels and adenylyl cyclase in cardiac myocytes. *J. Biol. Chem.* **272,** 19401-19407 (1997).
12. Carl, S.L. *et al.* Immunolocalization of sarcolemmal dihydropyridine receptor and sarcoplasmic reticular triadin and ryanodine receptor in rabbit ventricle and atrium. *J. Cell Biol.* **129,** 673-682, (1995).
13. Abriel, H., Rougier, J.S., & Jalife, J. Ion Channel Macromolecular Complexes in Cardiomyocytes: Roles in Sudden Cardiac Death. *Circ. Res.* **116,** 1971-1988 (2015).
14. Bourdin, B. *et al.* Molecular Determinants of the Cavb-induced Plasma Membrane Targeting of the Cav1.2 Channel. *J. Biol. Chem.* **285,** 22853-22863 (2010).
15. Raybaud, A. *et al.* The Role of the GX9GX3G Motif in the Gating of High Voltage-activated Calcium Channels. *J. Biol. Chem.* **281,** 39424-39436 (2006).
16. Burashnikov, E. *et al.* Mutations in the cardiac L-type calcium channel associated with inherited J-wave syndromes and sudden cardiac death. *Heart Rhythm.* **7,** 1872-1882 (2010).
17. Hennessey, J.A. *et al.* A CACNA1C Variant Associated with Reduced Voltage-Dependent Inactivation, Increased Cav1.2 Channel Window Current, and Arrhythmogenesis. *PLoS ONE.* **9,** e106982 (2014).
18. Adan, A., Alizada, G., Kiraz, Y., Baran, Y., & Nalbant, A. Flow cytometry: basic principles and applications. *Crit Rev Biotechnol.* 1-14 (2016).

19. Graham, M.D. The Coulter Principle: Foundation of an Industry. *J. Lab. Autom.* **8,** 72-81 (2003).
20. Baumgarth, N., & Roederer, M. A practical approach to multicolor flow cytometry for immunophenotyping. *J. Immunol. Methods*. **243,** 77-97 (2000).
21. Rothe, G. In: *Cellular Diagnostics. Basics, Methods and Clinical Applications of Flow Cytometry.* Sack U, Tarnok A, & Rothe G eds., Karger, Basel, 53-88 (2009).
22. Bourdin, B. *et al.* Functional Characterization of Cavalpha2delta Mutations Associated with Sudden Cardiac Death. *J. Biol. Chem.* **290,** 2854-2869 (2015).
23. Tetreault, M.P. *et al.* Identification of glycosylation sites essential for surface expression of the Cavalpha2delta1 subunit and modulation of the cardiac Cav1.2 channel activity. *J. Biol. Chem.* **291,** 4826-43, (2016).
24. Senatore, A., Boone, A.N., & Spafford, J.D. Optimized Transfection Strategy for Expression and Electrophysiological Recording of Recombinant Voltage-Gated Ion Channels in HEK-293T Cells. *J Vis Exp.* **47,**. (2011).
25. Herzenberg, L.A., Tung, J., Moore, W.A., Herzenberg, L.A., & Parks, D.R. Interpreting flow cytometry data: a guide for the perplexed. *Nat.Immunol.* **7,** 681-685 (2006).
26. Shakeri, B., Bourdin, B., Demers-Giroux, P.O., Sauve, R., & Parent, L. A quartet of Leucine residues in the Guanylate Kinase domain of Cavbeta determines the plasma membrane density of the Cav2.3 channel. *J Biol Chem.* **287,** 32835-32847 (2012).
27. Morton, R.A., Baptista-Hon, D.T., Hales, T.G., & Lovinger, D.M. Agonist- and antagonist-induced up-regulation of surface 5-HT3A receptors. *Br. J. Pharmacol.* **172,** 4066-4077 (2015).
28. Hoffmann, C. *et al.* Fluorescent labeling of tetracysteine-tagged proteins in intact cells. *Nat. Protocols.* **5,** 1666-1677 (2010).
29. Cockcroft, C.J. In: *Ion Channels: Methods and Protocols.* Gamper, N. ed., Humana Press, Totowa, NJ, 233-241, (2013).
30. Gonzalez-Gutierrez, G., Miranda-Laferte, E., Neely, A., & Hidalgo, P. The Src Homology 3 Domain of the beta-Subunit of Voltage-gated Calcium Channels Promotes Endocytosis via Dynamin Interaction. *J. Biol.Chem.* **282,** 2156-2162 (2007).
31. Galizzi, J.P., Borsotto, M., Barhanin, J., Fosset, M., & Lazdunski, M. Characterization and photoaffinity labeling of receptor sites for the Calcium channel inhibitors d-cis-diltiazem, (+/-)-bepridil, desmethoxyverapamil, and (+)-PN 200-110 in skeletal muscle transverse tubule membranes. *J. Biol.Chem.* **261,** 1393-1397, (1986).
32. Bezanilla, F. The voltage sensor in voltage-dependent ion channels. *Physiol.Rev.* **80,** 555-592, (2000).
33. Sigworth, F.J. The variance of sodium current fluctuations at the node of Ranvier. *J Physiol.* **307,** 97-129, (1980).
34. Bailey, M.A., Grabe, M., & Devor, D.C. Characterization of the PCMBS-dependent modification of KCa3.1 channel gating. *J. Gen. Physiol.* **136,** 367-387 (2010).
35. Fletcher, P.A., Scriven, D.R., Schulson, M.N., & Moore, E.D. Multi-Image Colocalization and Its Statistical Significance. *Biophys. J.* **99,** 1996-2005 , (2010).
36. Lizotte, E., Tremblay, A., Allen BG, & Fiset, C. Isolation and characterization of subcellular protein fractions from mouse heart. *Anal. Biochem.* **345,** 47-54 (2005).
37. Mattheyses, A.L., Simon, S.M., & Rappoport, J.Z. Imaging with total internal reflection fluorescence microscopy for the cell biologist. *J. Cell Sci.* **123,** 3621-3628 (2010).
38. Yamamura, H., Suzuki, Y., & Imaizumi, Y. New light on ion channel imaging by total internal reflection fluorescence (TIRF) microscopy. *J. Pharmacol. Sci.* **128,** 1-7 (2015).
39. Wible, B.A. *et al.* HERG-Lite-R: A novel comprehensive high-throughput screen for drug-induced hERG risk. *J. Pharmacol. Toxicol. Methods.* **52,** 136-145 (2005).
40. Wilde, A.A.M., & Brugada, R. Phenotypical Manifestations of Mutations in the Genes Encoding Subunits of the Cardiac Sodium Channel. *Circ. Res.* **108,** 884-897 (2011).
41. Milano, A. *et al.* Sudden Cardiac Arrest and Rare Genetic Variants in the Community. *Circ Cardiovasc Genet*. in press, (2016).
42. Schnell, U., Dijk, F., Sjollema, K.A., & Giepmans, B.N.G. Immunolabeling artifacts and the need for live-cell imaging. *Nat. Meth.* **9,** 152-158 (2012).

